# Semi-empirical calculation of solid surface tensions in body-centred cubic transition metals

PHILOSOPHICAL MAGAZINE A, 1986, VOL. 54, NO. 2, 301–315

# Semi-empirical calculation of solid surface tensions in body-centred cubic transition metals

By G. J. ACKLAND†‡ and M. W. FINNIS†

† Theoretical Physics Division, Building 424.4, Atomic Energy Research Establishment, Harwell, Oxfordshire OX11 ORA, England
‡ Department of Theoretical Physics, 1 Keble Road, Oxford OX1 3NP, England

[*Received 16 September 1985 and accepted 30 December 1985*]

ABSTRACT

We present calculations of surface tension (surface stress $\gamma$) for the body-centred cubic (b.c.c.) metals V, Nb, Ta, Mo and W made using simple empirical $N$-body potentials obtained by Finnis and Sinclair (1984). Results for several crystal faces are evaluated and compared with the corresponding surface energies $\sigma$. Although there is a broad correlation between the calculated tensions and energies for different metals, and the two quantities are of a similar order of magnitude, they differ from one another by a factor of up to 2. Variant potentials for molybdenum were constructed to test the sensitivity of the results; negative surface tensions were found in some cases and shown to be a symptom of metastability of the b.c.c. structure.

## § 1. INTRODUCTION

The present paper addresses the problem of calculating surface tensions in solid metals and compares the results obtained for several different transition metals and crystal faces. We believe that these are the first calculations of surface tension $\gamma$ (compared with surface energy $\sigma$) for solid metals which go beyond a pairwise interatomic force model. By surface tension we mean here the average tensile force acting across unit length of the surface. For surfaces which do not have threefold or fourfold symmetry, the force per unit length in the surface is anisotropic, and in such cases we define a surface stress tensor, of which the surface tension is the average diagonal component. These concepts are discussed in detail in § 2.

The interpretation of experimental data in the case of solids usually involves surface tensions and not surface energies (e.g. in zero-creep experiments) (Kumikov and Khokonov 1983, Bikerman 1965); thus it is arguably of greater importance to derive a theory of $\gamma$ than of $\sigma$. A further stimulus to the present work was provided by the recent observation of small bubbles of solid noble gases within the lattice structure of metals (Evans and Mazey 1985). A theoretical interpretation of the stresses in the matrix around such bubbles in relation to their internal pressure requires a value for their surface (or interfacial) tension rather than for surface energy. Although the matter has been clearly discussed (Gibbs 1931, Shuttleworth 1949, 1950, Bikerman 1965, Benson and Yun 1967, Zadumkin and Shebzukova 1969), one still often finds that no distinction is drawn between these two concepts, which in the case of liquids are identical, but which in solids are very different. We discuss briefly the formal theory in § 2. It turns out from the present calculations that $\sigma$ and $\gamma$, besides being conceptually

different, may differ numerically by a factor of about 2. We had no a priori reason even to expect $\gamma$ to have a positive sign, although we now suspect that the latter condition is necessary for stability of the crystal surface structure.

Numerous theoretical calculations have been made of surface energies $\sigma$ of b.c.c. transition metals. At the simplest level, pair-potential calculations have been made, but they are inevitably too unrealistic to be of use for quantitative, and sometimes qualitative, predictions. For example, they invariably predict an outward relaxation of the surface layer (see, for example, Benedek 1978) in contradiction to experiment, because they inadequately represent the d-band energy and its dependence on the atomic environment. Furthermore, the pair potentials which best represent the bulk properties of metals are non-equilibrium potentials, which required the addition of a volume-dependent term in the energy to satisfy the condition of zero pressure at the observed lattice spacing. There seems to be no satisfactory way of using such a model at a surface. At the other extreme, the most sophisticated calculations of surface energy are those of Fu, Ohnishi, Jansen and Freeman (1985), who employed a linear augmented plane wave (APW) theory to make self-consistent electronic structure calculations of Mo and V (100) surfaces, and evaluated the corresponding surface energies. Intermediate in complexity and computing cost are calculations based on the tight-binding approximation to model the d-band cohesion (Cyrot-Lackmann 1969, Desjonquères and Cyrot-Lackmann 1975, Treglia, Desjonquères and Spanjaard 1983, Masuda, Yamamoto and Doyama 1983). The tight-binding approximation can be simplified to an analytic second or fourth moment expansion for the d-electron density of states, or the recursion method (Haydock, Heine and Kelly 1972, Haydock 1980, Heine 1980, Kelly 1980) can be applied to include effects of higher moments in a continued-fraction expansion.

Relaxation of the atoms at the surface has not been explored in the APW method, and in the tight-binding methods it has been restricted to the surface layer, because of the complexity of the resulting potential energy functions and the limitations in computer power. While this is probably adequate for energy calculations, which are only slightly affected by relaxation (up to 5% according to our present calculations), the large effect of relaxation on surface tension which we find means that the relaxation of a number of layers is essential for calculating $\gamma$. In this paper we use the semi-empirical potentials of Finnis and Sinclair (FS), which were fitted to bulk properties. They are equivalent to second-moment approximations to the density of states and have a sufficiently simple form to allow relaxation of several surface layers. The results for $\sigma$ including relaxation have already been obtained with these potentials by Matthai and Bacon (1985). We consider surfaces (310) and (110) in addition to the (100) surface.

The plan of the paper is as follows. In § 2 we define the concept of surface tension in relation to surface energy. In § 3 we discuss the simple FS model for interatomic forces in the metals concerned, including a number of variant potentials in the case of molybdenum. Section 4 describes the method of calculating energies and tensions including the effect of surface relaxation by an energy minimization procedure. Results are presented in § 5 and the conclusions are summarized in § 6.

## § 2. Theory of surface tension

The distinction between the concepts of surface energy and surface tension in solids, which is central to our calculations, is not new (Gibbs 1931). It is not, however, widely acknowledged in the literature and to our knowledge all previous calculations which attempt to model the electronic structure of metals by going beyond pair potentials

have concentrated on the surface energy. We therefore explain the relationship between these concepts here. Realistic calculations of surface tension in solids have previously been confined to rare gas solids and ionic crystals (Shuttleworth 1950, Benson and Yun 1967, Tasker 1979) in which classical shell models or pairwise interatomic force models are a good description of the energetics. It should be pointed out that the following definitions and derivations should properly be made in terms of the Gibbs free energy; however, our calculations are restricted to the internal energy at zero temperature, and so we continue to refer simply to the energy.

The surface energy $\sigma$ of a solid is well known as the energy required to create unit area of new surface, e.g. by cleavage. It is an idealized concept, because in reality the creation of new surface involves dissipative processes such as dislocation generation and movement, which is why the work of fracture greatly exceeds the theoretical energy required for cleavage of a metal. The surface energy naturally depends on the crystal face created and includes the effect of relaxation of the surface layers of atoms from their bulk perfect lattice sites. The extensive quantity corresponding to the surface energy is referred to as the superficial energy; it is the surface energy multiplied by the surface area, i.e. $\sigma A$.

We now define the surface stress tensor $\tau_{\alpha\beta}$ as the strain derivative of the superficial energy, per unit area. We only consider homogeneous strains within the plane of the surface $\varepsilon_{\alpha\beta}$; $\alpha, \beta \in (x, y)$. Thus

$$\tau_{\alpha\beta} = A^{-1}\partial(\sigma A)/\partial\varepsilon_{\alpha\beta}. \tag{1}$$

Finally we define the surface tension as the average of the $x$ and $y$ tensile surface stresses:

$$\gamma = \tfrac{1}{2}(\tau_{xx} + \tau_{yy}). \tag{2}$$

$\gamma$ is therefore the derivative of the superficial energy with respect to a uniform isotropic stretching of the surface.

Although $\tau_{\alpha\beta}$ is formally similar to the bulk stress tensor, there is an important difference, namely, for a solid in equilibrium under no external loading, the stress in the bulk is assumed to vanish; however, the surface stress tensor does not in general vanish for, if an imaginary cut is made through a crystal perpendicular to the surface, there is a non-vanishing stress across the cut near the surface, which when integrated down several tens or hundreds of ångstroms gives the surface stress as defined above. Note that, if this integration of the normal stress across the cut is carried right through the crystal, the result is zero because the surface stress must be balanced by a bulk stress, the size of which tends to zero inversely as the thickness of the crystal. Considering for example a stretched wire of radius $r$, this bulk stress is

$$\gamma \times \text{circumference/area} = 2\gamma/r.$$

It must be balanced by the applied tensile stress before any creep occurs, which is how the surface tension, or more precisely the average surface stress, is measured by a zero-creep experiment.

The use in the literature of the term surface tension when surface energy is meant has been a source of some confusion. It originates because in liquids the two quantities are similar. Physically this is because as a liquid surface is stretched isothermally,

additional atoms move into surface positions and the structure of the surface, and hence $\sigma$, remains constant. Thus, for $xx$ or $yy$ strains in a liquid, eqn. (1) becomes

$$\begin{aligned}\tau_{\alpha\beta} &= \sigma A^{-1}\partial A/\partial\varepsilon_{\alpha\beta} \\ &= \sigma\delta_{\alpha\beta}.\end{aligned} \tag{3}$$

Hence

$$\gamma = \sigma.$$

Returning to the surface stress, for practical calculation in solids it is convenient to work with the energy $U_c$ per unit cell of the surface and the area $A_c$ per unit cell, so that eqn. (1) becomes

$$\tau_{\alpha\beta} = A_c^{-1}\partial U_c/\partial\varepsilon_{\alpha\beta}. \tag{4}$$

$U_c$ can be written as a sum of contributions from each site $u_i$:

$$U_c = \sum_i u_i.$$

In simple cases, this involves just one site per layer of atoms. Since $u_i$ tends to a constant (the cohesive energy) far from the surface, the sum over $u_i$ does not converge in a semi-infinite crystal. However, the sum over $\partial u_i/\partial\varepsilon_{\alpha\beta}$, which is needed to evaluate eqn. (4), does converge. Thus eqn. (4) becomes

$$\tau_{\alpha\beta} = A_c^{-1}\sum_i \partial u_i/\partial\varepsilon_{\alpha\beta}. \tag{5}$$

We can express eqn. (5) in a way more directly related to interatomic forces as follows. The strain derivative in eqn. (5) can be expressed in terms of derivatives with respect to interatomic distances from the relation

$$dR_{k\alpha} = \sum_\beta \varepsilon_{\alpha\beta}(R_{k\beta} - R_{i\beta}).$$

We obtain

$$\begin{aligned}\tau_{\alpha\beta} &= A_c^{-1}\sum_i\sum_k (R_{k\beta} - R_{i\beta})\partial u_i/\partial R_{k\alpha}, \\ &= -A_c^{-1}\sum_i\sum_k (R_{k\beta} - R_{i\beta})F_{ki\alpha}.\end{aligned} \tag{6}$$

The $k$ summation runs over all sites in the lattice. The final expression (6) introduces $\mathbf{F}_{ki}$, which we call the partial force on atom $k$ due to site $i$. We can think of the $k$ summation as defining a local stress at site $i$, which tends to the bulk stress per site far from the surface. The local stress defined in this way has been used by previous authors for studying the effect of defects by computer simulation (Egami and Vitek 1984). The partial force $\mathbf{F}_{ki}$ is pairwise only in a formal sense, because the functions $u_i$ are not linear combinations of atomic functions. For a simple pairwise potential model of the energy, we have

$$\mathbf{F}_{ki} = -\tfrac{1}{2}\nabla_k V(R_{ik}),$$

where

$$R_{ik}=|\mathbf{R}_k-\mathbf{R}_i|,$$

which is a truly pairwise description. However, in the FS model, which has the structure of an embedded-atom model (Daw and Baskes 1983), the partial forces acting between $i$ and $k$ depend on their local environment.

## § 3. The model

### 3.1. *The FS model*

In the calculations to be described, the model used was that derived by Finnis and Sinclair (1984) for the purpose of atomistic simulation. The model of the energy comprises a many-body term, which is attractive, and a repulsive pair potential. The form of these components is as follows.

The total energy of the configuration of atoms is written as

$$U_{\text{tot}}=U_N+\tfrac{1}{2}\sum_{ij}V(R_{ij}). \tag{7}$$

$U_N$ is the $N$-body term and the second term is a conventional pair-potential summation. The $N$-body term has the form

$$U_N=-A\sum_i\left(\sum_j\phi(R_{ij})\right)^{1/2}. \tag{8}$$

This represents the cohesion in the manner of a second-moment approximation to the tight-binding band energy, which gives rise to a cohesive energy varying as the square root of the atomic coordination.

The above energy functions were parameterized in a purely empirical way by FS; thus

$$\begin{aligned}\phi(r)&=(r-d)^2, && r\leqslant d,\\ &=0, && r>d.\end{aligned}$$

and

$$\begin{aligned}V(r)&=(r-c)^2(c_0+c_1r+c_2r^2), && r\leqslant c,\\ &=0, && r>c,\end{aligned}$$

where the cut-offs $d$ and $c$ were taken to lie between the second- and third-neighbour separations; these and the other parameters $A$, $c_0$, $c_1$ and $c_2$ were fitted to the experimental cohesive energy, lattice parameter and three elastic moduli. The remaining sixth degree of freedom in the fitting was used to ensure that the unrelaxed vacancy formation energy as in the range of observed values. We note here that the fitted potential parameters for iron in FS are incorrect (Finnis and Sinclair 1986).

The energy is easy to compute. Compared with a purely pairwise energy, it is necessary simply to perform an extra lattice summation to obtain the quantities

$$\rho_i=\sum_j\phi(R_{ij}).$$

The total energy is then a sum of site energies $u_i$, where

$$u_i=-A\rho_i+\tfrac{1}{2}\sum_j V(R_{ij}). \tag{9}$$

Before relaxation the surface energy is composed of changes from their bulk values of the site energies within those few layers near the surface in which atoms have an incomplete set of first or second neighbours. These include only the top layer for (110), two layers for (100) and three layers for (310). To perform a relaxation, however, which is particularly important for the calculation of $\gamma$, the forces are required, which in the FS model are influenced by sixth neighbours, i.e. from $\langle 111 \rangle$ to $\langle 004 \rangle$, or (in general configurations) out to a range $2d$. The total force on atom $i$ is given by

$$\mathbf{F}_i = \mathbf{F}_{ii} + \sum_{k \neq i} \mathbf{F}_{ik}, \tag{10}$$

where

$$\mathbf{F}_{ii} = \tfrac{1}{2} A \rho_i^{-1/2} \sum_{k \neq i} \nabla_i \phi(|\mathbf{R}_i - \mathbf{R}_k|) \tag{11}$$

and

$$\mathbf{F}_{ik} = \tfrac{1}{2} A \rho_k^{-1/2} \nabla_i \phi(|\mathbf{R}_i - \mathbf{R}_k|) - \nabla_i V(|\mathbf{R}_i - \mathbf{R}_k|). \tag{12}$$

The force $\mathbf{F}_{ik}$ on $i$ is influenced by atoms out to twice the cut-off in $\phi$ because the change in $\rho$ induced at a site $k$ by the movement of an atom $i$, which is within a range $d$ of $k$, changes the site energy at $k$ by an amount which depends on the original value of $\rho$ at $k$, which in turn depends on the position of all its own neighbours within the range $d$.

### 3.2. *Molybdenum variants*

The parameterization of the FS model is not unique. The actual values depend on the choice of a physically reasonable vacancy formation energy, for which there is more experimental uncertainty than for the fitted bulk properties, To explore the sensitivity to this choice of parameters, for the case of molybdenum a family of potentials has been constructed, each with different values of vacancy formation energy. The parameters are shown in table 1. Each of these was used to evaluate surface energies, tensions and relaxations.

## §4. Calculations

### 4.1. *Surface stress*

The energy of the surface was minimized by allowing the top 16 interlayer spacings to vary until the forces on each atom fell to below $10^{-11}$ eV Å$^{-1}$. A variable metric algorithm was used (Norgett and Fletcher 1970). The structure of each layer was held constant and no lateral movement of the layers was allowed. In the final relaxed position the structure of the layers was found to be a minimum with respect to lateral movement in all directions, except in the case of the variant molybdenum potentials III–VII for which the b.c.c. structure is only metastable. Once the final layer separations had been found, the relaxed surface tensions $\gamma$ were calculated by analytic differentiation of the energy function with respect to the area. This was carried out by evaluating and summing the contributions of individual layers as well as by evaluating the expressions with all the layers simultaneously strained. The results of evaluating the analytic formula were verified by numerical differentiation of the surface energy, which is the approach that one might use for more complicated energy functions.

In the case of the (110) and (310) surfaces the surface stress is not isotropic, since the fourfold symmetry of the (100) surface is lacking. The two principal tensions $\tau_{xx}$ and $\tau_{yy}$,

Table 1. Variant fitting parameters for molybdenum.

| | I | II | III | IV | V | VI | VII |
|---|---|---|---|---|---|---|---|
| $d$ | 4·11482492 | 4·13527148 | 4·15448345 | 4·15702013 | 4·15970733 | 4·16255842 | 4·16558841 |
| $A$ | 1·88711660 | 1·91549423 | 1·94220263 | 1·94573221 | 1·94947198 | 1·95344071 | 1·95765943 |
| $c$ | 3·25 | 3·27 | 3·28 | 3·281 | 3·282 | 3·283 | 3·284 |
| $c_0$ | 43·44752148 | 68·96804405 | 91·64459247 | 94·60560112 | 97·73810380 | 101·05802567 | 104·58332891 |
| $c_1$ | −31·93329757 | −51·74177184 | −69·36150859 | −71·6627446 | −74·09734771 | −76·67769904 | −79·4177634 |
| $c_2$ | 6·08042486 | 9·91756084 | 13·34036947 | 13·78772813 | 14·26106998 | 14·76280613 | 15·29565607 |

Fig. 1

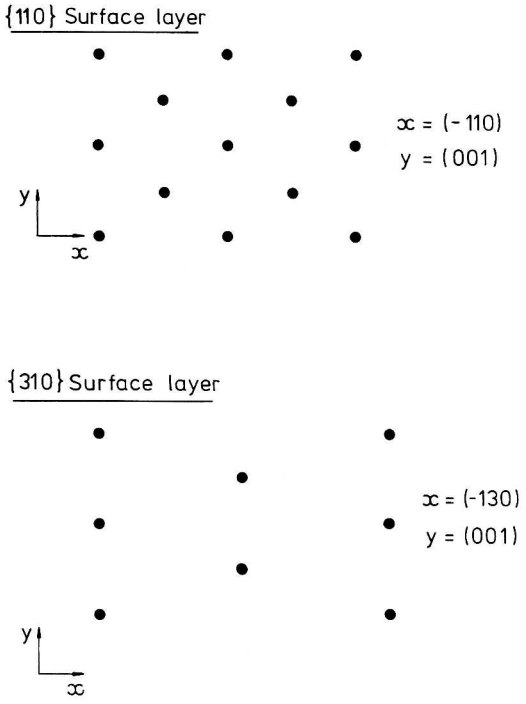


The definition of the $x$ and $y$ directions in the (100) and (310) surfaces.

in the directions shown in fig. 1, were therefore also evaluated by direct analytic differentiation of the energy with respect to the components of the interatomic separation in these directions (see eqns. (6) and (12)) For these cases it was verified that the independently calculated $\tau_{xx}$, $\tau_{yy}$ and $\gamma$ satisfied eqn. (2).

### 4.2. *Structural stability*

One of the most important criteria in choosing a potential is that the stable crystal structure should be that observed in nature. It is also a particularly difficult criterion to test exhaustively. Whilst the fit to the elastic moduli ensures that the body-centred cubic (b.c.c.) structure is at least metastable for the FS models, there is no guarantee that a crystal structure of lower energy does not exist. To check this possibility, the binding energy per atom within a b.c.c. lattice was evaluated and compared with that for several other plausible crystal structures, namely face-centred cubic (f.c.c.), hexagonal close-packed (h.c.p.) (=f.c.c. energy for the FS models), A15 ($\beta$-W), C14 ($MgZn_2$), C15 ($MgCu_2$) and C36 ($MgNi_2$). In addition the $c/a$ ratio and the volume of the b.c.c. cell were scanned over a wide range; the f.c.c. structure is the special case of $c/a = 2^{1/2}$. In all cases, except the variant molybdenum potentials III–VII, the b.c.c. structure had the lowest energy, which gives reassurance, even if not certainty, that it is absolutely the most stable structure.

For the variant molybdenum potentials III–VII, the true minimum was found to be a body-centred tetragonal (b.c.t.) structure (see fig. 2), which is obtained by reducing one side of the b.c.c. unit cell until it becomes equal to the nearest-neighbour spacing, and reducing the unit cell volume slightly. The atoms thereby get ten nearest neighbours

Fig. 2

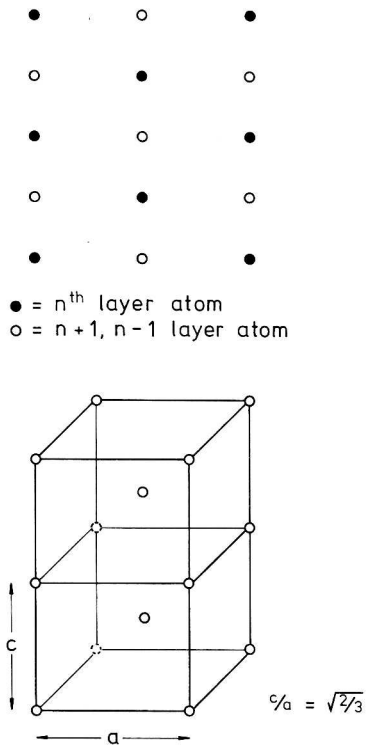


The stable structure of the variant molybdenum potentials III–VII: (*a*) viewed as stacked close-packed planes; (*b*) viewed as a b.c.t. structure.

and four second neighbours This instability of the b.c.c. structure correlates with the negative surface tensions shown by these variants, as we discuss in § 5.

### 4.3. *Surface reconstruction*

Much experimental and theoretical work has been done recently to elucidate the nature and mechanism of the reconstruction observed on the tungsten and molybdenum (100) surfaces (Debe and King 1977, Masuda, Hamada and Terakura 1984, Terakura, Terakura and Hamada 1981, Treglia *et al.* 1983). The explanation appears to lie in details of the electronic structure which we do not expect to be contained in the simple FS model; nevertheless our study would have been incomplete without establishing whether any reconstruction is predicted by the model. We calculated the stability of a fully relaxed tungsten surface with respect to the rearrangement modes proposed by Masuda *et al.*, with the result that for the FS model the surface is most stable in the unreconstructed state.

## § 5. Discussion of results

Results of the relaxation of the three faces of the different metals are presented as follows: table 2 shows the amount by which each layer separation changes as a result of the relaxation; table 3 shows the relaxed surface energies $\sigma$ and tensions $\gamma$ and compares

Table 2. Movement of upper layers on relaxation. Negative values show inward relaxation of the surface.

| | Vanadium | | Niobium | | Tantalum | | Molybdenum | | Tungsten | |
|---|---|---|---|---|---|---|---|---|---|---|
| | $\Delta(\times 10^{-4}$ Å) | | $\Delta(\times 10^{-4}$ Å) | | $\Delta(\times 10^{-4}$ Å) | | $\Delta(\times 10^{-4}$ Å) | | $\Delta(\times 10^{-4}$ Å) | |
| {100}, layer 1 | −984 | −6·9% | −2205 | −16·0% | −560 | −3·5% | −429 | −2·8% | −120 | −0·8% |
| {100}, layer 2 | +34 | +0·3% | +635 | +3·9% | −169 | −1·0% | −45 | −0·2% | −108 | −0·7% |
| {100}, layer 3 | +13 | −0·1% | −241 | −1·5% | +59 | +0·4% | +13 | +0·1% | +25 | +0·2% |
| {100}, layer 4 | −2 | | +114 | +0·7% | −10 | | −3 | | −6 | |
| Total | −939 | | −1734 | | −678 | | −463 | | −207 | |
| {110}, layer 1 | −802 | −3·9% | −1231 | −5·1% | −637 | −2·8% | −323 | −1·5% | −259 | −1·2% |
| {110}, layer 2 | +87 | +0·4% | +199 | +0·9% | +49 | +0·2% | +11 | | +6 | |
| {110}, layer 3 | −9 | | −32 | −0·1% | +4 | | | — | | — |
| {110}, layer 4 | +1 | | −5 | | | — | | — | | — |
| Total | −723 | | −1069 | | −584 | | −312 | | −253 | |
| {310}, layer 1 | −1846 | −19·2% | −2950 | −29·4% | −1510 | −15·2% | −803 | −8·1% | −605 | −6·0% |
| {310}, layer 2 | +323 | +3·4% | −266 | −2·6% | +512 | +5·2% | +135 | +1·4% | +235 | +2·3% |
| {310}, layer 3 | −284 | −3·0% | +466 | +4·5% | −550 | −5·6% | −214 | −2·2% | −263 | −2·6% |
| {310}, layer 4 | +28 | +0·3% | −245 | −2·5% | +183 | ×1·8% | +55 | +0·5% | +71 | +0·7% |
| {310}, layer 5 | +98 | +1·0% | +96 | +1% | +6 | | +18 | | +5 | |
| Total | −1727 | | −2937 | | −1375 | | −823 | | −567 | |

them with the unrelaxed values; table 4 shows the principal components of the surface stress tensor for the (110) and (310) planes.

Considering the magnitude of the surface relaxation, we see from table 2 that it varies considerably between the metals. However, in all cases the relaxation of the surface layer is inwards, and there is a contraction of the outermost interplanar spacing.

Experimentally this is what is found by low-energy electron diffraction (LEED) (Ignatiev, Jona, Shih, Jepsen and Marcus 1975, Van Hove and Tong 1976, Debe, King and Marsh 1977, Debe and King 1979, Clarke 1980) for Mo and W. The results presented here are rather smaller than the experimental contractions; Clarke (1980) finds a contraction in molybdenum (100) of 9·5% while Ignatiev *et al.* (1975) find 11·5%. In tungsten there is a wide range of experimental results ranging from 4·4% (Debe *et al.* 1977) up to 11% (Lee, Ignatiev, Tong and Van Hove 1977), again larger than observed here. For vanadium, Jensen, Andersen, Nielsen and Adams (1982) observe a first-layer contraction of 7% and a small expansion of the second-layer separation, exactly as predicted by the model. In tantalum a surface contraction of 11% and a second-layer expansion of 1% has been observed (Titov and Moritz 1982); again the FS model predicts a smaller effect.

It should be noted that, while large values for the surface contraction are found in LEED experiments, results from ion scattering tend to suggest smaller contractions, typically less than 6% for tungsten (Clarke 1980), and so there is still some uncertainly about the experimental situation. The calculated contractions in the molybdenum variants increase quite substantially (II, which is stable b.c.c., contracts by 5·6% and VII by 14·0%), showing that this feature is quite sensitive to the chosen parameters. It has also been shown experimentally that the contraction of the (100) surface is considerably greater than that of the (110) (King and Woodruff 1981), which is as predicted in these calculations.

Table 3. Contributions to total surface tension and surface energy from upper layers.

| | Vanadium | | Niobium | | Tantalum | | Molybdenum | | Tungsten | |
|---|---|---|---|---|---|---|---|---|---|---|
| | $\gamma$ (mJ m$^{-2}$) | $\sigma$ (mJ m$^{-2}$) | $\gamma$ (mJ m$^{-2}$) | $\sigma$ (mJ m$^{-2}$) | $\gamma$ (mJ m$^{-2}$) | $\sigma$ (mJ m$^{-2}$) | $\gamma$ (mJ m$^{-2}$) | $\sigma$ (mJ m$^{-2}$) | $\gamma$ (mJ m$^{-2}$) | $\sigma$ (mJ m$^{-2}$) |
| {100}, layer 1 | 2670 | 1470 | 2893 | 1630 | 3575 | 1994 | 2404 | 1800 | 3058 | 2513 |
| {100}, layer 2 | −210 | 282 | −382 | 352 | −225 | 350 | −121 | 305 | 52 | 414 |
| {100}, layer 3 | −45 | −20 | 33 | −39 | −123 | −12 | −46 | −4 | −89 | — |
| {100}, layer 4 | 8 | 1 | −22 | 15 | 24 | −7 | +5 | −1 | 13 | — |
| Total { Unrelaxed | (3470) | (1761) | (4474) | (2046) | (4330) | (2345) | (3029) | (2112) | (3465) | (2926) |
| Total { Relaxed | 2424 | 1733 | 2532 | 1956 | 3249 | 2328 | 2241 | 2100 | 3032 | 2924 |
| {110}, layer 1 | 1513 | 1460 | 1902 | 1644 | 1877 | 1969 | 1673 | 1824 | 1582 | 2571 |
| {110}, layer 2 | −455 | 13 | −773 | 24 | −444 | 11 | −285 | 5 | −259 | 4 |
| {110}, layer 3 | 48 | — | 122 | 1 | 33 | — | 9 | — | 6 | — |
| {110}, layer 4 | −5 | — | −20 | — | −3 | — | 0 | — | −1 | — |
| Total { Unrelaxed | (2059) | (1499) | (2928) | (1718) | (3131) | (2003) | (1982) | (1839) | (1872) | (2582) |
| Total { Relaxed | 1101 | 1473 | 1235 | 1669 | 1463 | 1980 | 1397 | 1829 | 1328 | 2575 |
| {310}, layer 1 | 1208 | 1076 | 1253 | 1217 | 1600 | 1563 | 1177 | 1303 | 1404 | 1908 |
| {310}, layer 2 | 859 | 500 | 990 | 575 | 1097 | 724 | 735 | 583 | 885 | 866 |
| {310}, layer 3 | −167 | 183 | −292 | 238 | −192 | 242 | −101 | 187 | −47 | 267 |
| {310}, layer 4 | −104 | −16 | −162 | −16 | −116 | −22 | −80 | −3 | −73 | −8 |
| {310}, layer 5 | −11 | 4 | 41 | −5 | −41 | 14 | −20 | 2 | −33 | 6 |
| Total { Unrelaxed | (2980) | (1810) | (3945) | (2093) | (3645) | (2568) | (2675) | (2192) | (2895) | (3049) |
| Total { Relaxed | 1795 | 1745 | 1837 | 2014 | 2366 | 2512 | 1715 | 2070 | 2142 | 3036 |

Table 4. Principal surface stresses. The definitions of the $x$ and $y$ directions are shown in fig. 2.

| | Vanadium | | Niobium | | Tantalum | | Molybdenum | | Tungsten | |
|---|---|---|---|---|---|---|---|---|---|---|
| | $\tau_{xx}$ (mJ m$^{-2}$) | $\tau_{yy}$ (mJ m$^{-2}$) | $\tau_{xx}$ (mJ m$^{-2}$) | $\tau_{yy}$ (mJ m$^{-2}$) | $\tau_{xx}$ (mJ m$^{-2}$) | $\tau_{yy}$ mJ m$^{-2}$) | $\tau_{xx}$ (mJ m$^{-2}$) | $\tau_{yy}$ (mJ m$^{-2}$) | $\tau_{xx}$ (mJ m$^{-2}$) | $\tau_{yy}$ (mJ m$^{-2}$) |
| {110}, layer 1 | 2320 | 705 | 2742 | 1062 | 2987 | 766 | 2288 | 1057 | 2657 | 507 |
| {110}, layer 2 | −423 | −486 | −670 | −875 | −585 | −402 | −277 | −292 | −277 | −241 |
| {110}, layer 3 | +45 | +50 | 111 | 132 | 37 | 30 | 8 | 11 | 6 | 6 |
| {110}, layer 4 | −5 | −5 | −18 | −22 | −3 | −2 | — | — | — | — |
| Total | 1939 | 263 | 2168 | 301 | 2535 | 392 | 2019 | 775 | 2385 | 271 |
| {310}, layer 1 | 1644 | 772 | 1695 | 811 | 2198 | 1002 | 1602 | 752 | 1980 | 829 |
| {310}, layer 2 | 920 | 798 | 1083 | 897 | 1150 | 1034 | 796 | 674 | 944 | 825 |
| {310}, layer 3 | −144 | −190 | −280 | −304 | −153 | −229 | −76 | −126 | −10 | −83 |
| {310}, layer 4 | −81 | −124 | −139 | −184 | −93 | −139 | −58 | −102 | −50 | −96 |
| {310}, layer 5 | −15 | −7 | 44 | 37 | −46 | −25 | −25 | −15 | −40 | −26 |
| Total | 2335 | 1255 | 2405 | 1267 | 3085 | 1647 | 2247 | 1184 | 2833 | 1450 |

Table 5. Contributions to total surface tension from upper layers for variant molybdenum potentials.

| | Surface tension contribution ($mJ\,m^{-2}$) | | | | | | |
|---|---|---|---|---|---|---|---|
| | I | II | III | IV | V | VI | VII |
| {100}, layer 1 | 2404 | 1168 | −406 | −798 | −1267 | −1776 | −2233 |
| {100}, layer 2 | −121 | −557 | −1782 | −2283 | −2960 | −3869 | −5369 |
| {100}, layer 3 | −46 | −68 | −418 | −641 | −1001 | −1667 | −3579 |
| {100}, layer 4 | +5 | 9 | 42 | 41 | 21 | −80 | −794 |
| Total | 2241 | 542 | −2557 | −3674 | −5211 | −7396 | −11960 |
| {110}, layer 1 | 1673 | 1989 | 2271 | 2348 | 2348 | 2388 | 2433 |
| {110}, layer 2 | −285 | −284 | −283 | −282 | −282 | −281 | −280 |
| {110}, layer 3 | 9 | 9 | 9 | 9 | 9 | 9 | 9 |
| Total | 1397 | 1715 | 2002 | 2035 | 2074 | 2117 | 2160 |
| {310}, layer 1 | 1177 | 787 | 373 | 304 | 220 | 110 | −63 |
| {310}, layer 2 | 735 | 470 | 211 | 171 | 121 | 58 | −40 |
| {310}, layer 3 | −101 | −233 | −410 | −449 | −500 | −573 | −704 |
| {310}, layer 4 | −80 | −106 | −158 | −170 | −187 | −213 | −265 |
| Total | 1715 | 914 | −2 | −167 | −373 | −661 | −1153 |

The values of $\gamma$ and $\sigma$ are compared in table 3. The results for $\sigma$ and the relaxations are close to those found by Matthai and Bacon (1985) with these potentials, confirming the accuracy of all our calculations. We see firstly that $\gamma$ and $\sigma$ are of a similar order of magnitude. For the lowest-energy face, which is always the close-packed (110) face as expected, $\gamma$ is always less than $\sigma$, the greatest difference being for tungsten, where $\gamma = 1328\,mJ\,m^{-2}$ and $\sigma = 2575\,mJ\,m^{-2}$. For the (100) face which is next lowest in energy (with the exception of molybdenum, in which relaxation just makes (310) lower in energy than (100)) the trend is reversed and $\gamma > \sigma$. Vanadium has $\gamma$ slightly greater than $\sigma$ also for (310); for the other metals, on (310) $\gamma$ is less than $\sigma$, as on (110).

As table 4 shows, the surface stress is highly anistropic on the (110) and (310) surfaces, being lower along the close-packed directions. The extreme cases are on the (110) face, which has the lowest values of $\tau_{yy}$: below $300\,mJ\,m^{-2}$ in vanadium and tungsten. These low values are responsible for the relatively lower value of $\gamma$ compared with $\sigma$ on these faces.

The same calculations were made with the molybdenum variant potentials, and it was found that the surface tension after relaxation varies enormously both in sign and magnitude between these alternative potentials. The results are shown in table 5. A negative surface tension encourages larger interatomic separations between atoms within a layer and might be expected therefore to cause buckling of the surface. A full molecular dynamic simulation would be needed to examine this effect. In the present cases the b.c.c. structure was found to be only metastable whenever negative surface tensions were observed, indicating that the large surface relaxations in these cases were a highly constrained attempt to approach a lower-energy crystal structure. It is not surprising that in the presence of a defect, such as a surface, a metastable potential may lead to large distortions as the atoms try to rearrange to the true stable structure. The most useful molybdenum potential, for which the b.c.c. structure is the most stable, turned out to be the one already published, which also has the highest value of vacancy formation energy.

## § 6. Conclusions

We have elucidated in this paper the concepts of surface tension and surface stress as applied to solid metals and we have made a number of simple model calculations to illustrate the concepts.

The surface tensions of the transition metals are calculated to be of similar order of magnitude to their surface energies, rather larger in the (100) plane and smaller in the (310) and (110) planes, but always within a factor of 2. A comparison of contributions from each layer shows that the tension falls to zero rather less rapidly than the energy does. This is to be expected as the differential quantities that contribute to the surface stresses have a longer range than the components of the site energy. The surface stresses are highly anistropic on the faces with twofold symmetry, in the extreme cases (e.g. tungsten (110)) being almost an order of magnitude lower in the looser-packed directions.

As expected, the relaxation process has a much greater effect on the tensions than on the energies; in some cases the relaxed value is less than half the unrelaxed value. This illustrates why it is important to relax several layers, since any inaccuracy in surface relaxation would cause a much greater error in the surface tension than in the surface energy.

One of the most interesting observations is the large difference between the surface stresses in the different surfaces of the same element, which are much more pronounced than the variations in surface energy, particularly if the separate components of the surface stress tensor are compared. Experiments only provide a single value for the surface tension and the large spread of experimental results may be partly due to the proportion of various surfaces present. In a survey of experimental data (Kumikov and Khokonov 1983) it has been found that the scatter of experimental results is to a factor of up to 3; this is consistent with the variation expected from our calculations due to difference in surface tension between various surfaces and directions. Experimental factors not accounted for here include the contribution to the creep rate or surface stress of grain boundaries at the surface, and the increase in surface tension due to uneven surfaces (see Bikerman 1965).

Also significant is the difference between the surface relaxations of different elements. It might be expected that with potentials derived by the same procedure the relaxations of the upper layers would be similar, but in fact the total inward relaxation distance varies by a factor of up to 10 between the same crystal faces of different elements.

Our experience with the variant potentials for molybdenum suggests two further conclusions. Firstly, the stability of the observed crystal structure was a necessary condition for a positive surface tension. This is plausible as a general theorem, although we have no general proof. Secondly, the numerical results are very sensitive to the parameters of the potential; in view of the very simple nature of our potential model we would therefore emphasize our qualitative conclusions rather than attaching great significance to our precise numerical results, although the latter probably represent the best available estimates of surface tension in metals.

## References

Benedek, R., 1978, *J. Phys.* F, **8**, 1119.

Benson, G. C., and Yun, K. S., 1967, *The Solid–Gas Interface I*, edited by E. A. Flood (London: Edward Arnold), p. 203.

BIKERMAN, J. J., 1965, *Phys. Stat. Sol.*, **10,** 3.
CLARKE, L. J., 1980, *Surf. Sci.*, **91,** 131.
CYROT-LACKMANN, F., 1969, *Surf. Sci.*, **15,** 535–548.
DAW, M. S., and BASKES, M. I., 1983, *Phys. Rev. Lett.*, **50,** 1285.
DEBE, M. K., and KING, D. A., 1977, *Phys. Rev. Lett.*, **39,** 708; 1979, *Surf. Sci.*, **81,** 193.
DEBE, M. K., KING, D. A., and MARSH, F. S., 1977, *Surf. Sci.*, **68,** 437.
DESJONQUERES, M. C., and CYROT-LACKMANN, F., 1975, *J. Phys.* F, **5,** 1368.
EGAMI, T., and VITEK, V., 1984, *J. non-crystalline Solids*, **61 & 62,** 499.
EVANS, J. H., and MAZEY, D. J., 1985, *J. Phys.* F, **15,** L1.
FINNIS, M. W., and SINCLAIR, J. E., 1984, *Phil. Mag.* A, **50,** 45; 1986, *Phil. Mag.* A, **53,** 161.
FU, C. L., OHNISHI, S., JANSEN, H. J. F., and FREEMAN, A. J., 1985, *Surf. Sci.*, **82,** 425.
GIBBS, J. W., 1931, *Collected Works*, Vol. I (New York: Longmans, Green).
HAYDOCK, R., 1980, *Solid St. Phys.*, **35,** 215.
HAYDOCK, R., HEINE, V., and KELLY, M. J., 1972, *J. Phys.* C, **5,** 2845.
HEINE, V., 1980, *Solid St. Phys.*, **35,** 1.
IGNATIEV, A., JONA, F., SHIH, H, D., JEPSEN, D. W., and MARCUS, P. M., 1975, *Phys. Rev.* B, **11,** 4787.
JENSEN, V., ANDERSON, J. N., NIELSEN, H. B., and ADAMS, D. L., 1982, *Surf. Sci.*, **116,** 66.
KELLY, M. J., 1980, *Solid St. Phys.*, **35,** 296.
KING, D. A., and WOODRUFF, D. P., 1981, *The Chemical Physics of Solid Surfaces and Heterogeneous Catalysis*, Vol. 1, *Clean Solid Surfaces* (Amsterdam: Elsevier), p. 162.
KUMIKOV, V. K., and KHOKONOV, Kh. B., 1983, *J. Appl. Phys.*, **54,** 1346.
LEE, B. W., IGNATIEV, A., TONG, S. W., and VAN HOVE, M. A., 1977, *J. vac. Sci. Technol.*, **14,** 291.
MASUDA, K., HAMADA, N., and TERAKURA, K., 1984, *J. Phys.* C, **17,** L272.
MASUDA, K., YAMAMOTO, R., and DOYAMA, M., 1983, *J. Phys.* F, **13,** 1407.
MATTHAI, C. C., and BACON, D. J., 1985, *Phil. Mag.* A, **52,** 1.
NORGETT, M. J., and FLETCHER, R., 1970, *J. Phys.* C, **3,** L190.
SHUTTLEWORTH, R., 1949, *Proc. phys. Soc.* A, **62,** 167; 1950, *Proc. R. Soc.* A, **63,** 444.
TASKER, P. W., 1979, *Phil. Mag.* A, **39,** 119.
TERAKURA, I., TERAKURA, K., and HAMADA, N., 1981, *Surf. Sci.*, **111,** 479.
TITOV, A., and MORITZ, W., 1982, *Surf. Sci.*, **123,** L709.
TREGLIA, G., DESJONQUERES, M. C., and SPANJAARD, D., 1983, *J. Phys.* C, **16,** 2407.
VAN HOVE, M. A., and TONG, S. Y., 1976, *Surf. Sci.*, **54,** 91.
ZADUMKIN, S. N., and SHEBZUKOVA, I. G., 1969, *Physics Metal Metallogr., Wash.*, **28,** 3, 434.